

Low-Phase-Noise Tenfold Frequency Multiplication Based on Integrated Optical Frequency Combs

Eduardo Saia Lima¹, Nicola Andriolli², Senior Member, IEEE, Evandro Conforti¹, Life Senior Member, IEEE, Giampiero Contestabile, and Arismar Cerqueira Sodr , Jr.¹

Abstract—We experimentally demonstrate a low-phase-noise tenfold frequency multiplier based on a compact integrated optical frequency comb (OFC) generator. The Indium Phosphide (InP) monolithically integrated OFC is based on a flexible scheme using cascaded optical modulators. The extremely compact frequency multiplier is broadly tunable in wavelength and in OFC repetition frequency, making it interesting for high-spectral-purity mm-waves applications. OFC generation with a 2.6 GHz spacing and 19 tones within a 10 dB power range and an optical signal-to-noise ratio (OSNR) higher than 40 dB is reported. Using a 74 GHz-bandwidth photodetector, we achieve a set of 2.6 GHz phase-stabilized electrical tones, reaching carriers up to 39 GHz with a high signal-to-noise ratio (SNR). In particular, the OFC-based tenfold-multiplied signal (26 GHz) provides a remarkable low-phase-noise feature, equivalent to the commercially available radiofrequency (RF) generator used as a source at the same electrical power. At 26 GHz, phase-noise of -50 dBc/Hz and -80 dBc/Hz are reported for 10 Hz and 1 kHz offsets, respectively. The proposed system enables frequency multiplication up to 12-times without phase impairments, i.e., phase noise performance equivalent to a commercial RF generator, validating its potential to low-phase-noise and high-spectral-purity mm-wave applications.

Index Terms—5G, mm-waves, optical frequency comb (OFC), photonic integrated circuits (PIC).

I. INTRODUCTION

USE cases of the fifth-generation (5G) of mobile networks encompass enhanced mobile broadband (eMBB), ultra-reliable low-latency communication (uRLLC), and massive machine-type communication (mMTC) [1]. To this aim 5G new radio (5G NR) radio access network (RAN) has been standardized and the commercial deployment already started

Manuscript received 18 December 2021; revised 21 June 2022; accepted 30 June 2022. Date of publication 13 July 2022; date of current version 3 August 2022. This work was supported in part by the Rede Nacional de Ensino e Pesquisa (RNP)-Minist rio da Ci ncia, Tecnologia e Inova es e Comunica es (MCTIC) through the 6G Project under Grant 01245.010604/2020-14, in part by the Conselho Nacional de Desenvolvimento Cient fico e Tecnol gico (CNPq), in part by the Coordena o de Aperfei amento de Pessoal de N vel Superior (CAPES), in part by the Financiadora de Estudos e Projetos (FINEP), in part by the Funda o de Amparo   Pesquisa do Estado de Minas Gerais (FAPEMIG), and in part by the Italian Ministry of University and Research (MUR) through the PON R&I project QUANCOM. (Corresponding author: Arismar Cerqueira Sodr , Jr.)

Eduardo Saia Lima and Arismar Cerqueira Sodr , Jr., are with the Laboratory WOCA (Inatel), Santa Rita do Sapuca  37540-000, Brazil (e-mail: elima@get.inatel.br; arismar@inatel.br).

Nicola Andriolli is with the CNR—IEIIT, 56122 Pisa, Italy.

Evandro Conforti is with the DECOM—University of Campinas, Campinas 13083-970, Brazil.

Giampiero Contestabile is with Scuola Superiore Sant’Anna, 56124 Pisa, Italy.

Color versions of one or more figures in this letter are available at <https://doi.org/10.1109/LPT.2022.3189950>.

Digital Object Identifier 10.1109/LPT.2022.3189950

worldwide, initially on a non-standalone (NSA) operation mode based on the 4G control plane, and later on a standalone (SA) implementation, enabling all 5G features. Two distinct frequency ranges have been standardized, namely frequency range 1 (FR1) from 410 MHz to 7.125 GHz, and frequency range 2 (FR2) between 24.25 and 52.6 GHz [2]. In particular, the large spectrum of FR2, belonging to the millimeter waves (mm-waves) [3], enables Gbit/s communication employing bandwidths up to 400 MHz [4].

Millimeter-wave signals with high spectral purity and low phase noise are mandatory in several applications, such as wireless communications, radar, and spectroscopic sensing [5]. Typically, electronic synthesized radio frequency (RF) generators are used, which can be bulky and expensive, especially in the mm-waves range. Consequently, several techniques to generate low-phase-noise and frequency-tunable mm-waves in the optical domain have been reported, such as external modulation [6], optical injection locking (OIL) [7], and optical phase-locked loop (OPLL) [8]. In particular, external modulation based on phase modulators (PMs) and Mach-Zehnder modulators (MZMs) has demonstrated potential to provide generation and frequency multiplication with low phase noise and high tunability [9]. For instance, optical frequency doubling and quadrupling can be achieved using one modulator [10], while frequency quadrupling, sextupling, or octupling based on MZMs are also reported [9].

The mechanism behind the photonics-based mm-wave generation is the heterodyne detection, which demands high-phase correlation between the optical carriers. In this way, optical frequency combs (OFCs) based on external modulators provide phase-stabilized optical carriers, enabling low-noise RF signals generation with high-frequency tunability [11]. With respect to alternative optical frequency comb generation schemes, such as mode-locked lasers, micro ring modulators, or injection-locked lasers, the use of cascaded modulators schemes offer higher flexibility in terms of selection of both wavelength and frequency repetition rate [12].

In this context, our photonic integrated optical frequency comb generator based on cascaded modulators exploiting a monolithic integration in an Indium phosphide (InP) platform has been recently reported [12]. Photonic integration provides extremely compact and flexible optical frequency combs, enabling the central wavelength, frequency spacing and optical output power adjustment by controlling the photonic integrated circuit (PIC): a wavelength-tunable laser can be used for controlling the comb wavelength, a semiconductor optical amplifier (SOA) adjusts the output power, while the frequency spacing can be broadly tuned by an external RF generator at a relatively low frequency. An ad-hoc combination of the modulating signals can also be exploited in order to perform frequency line multiplication when required [13].

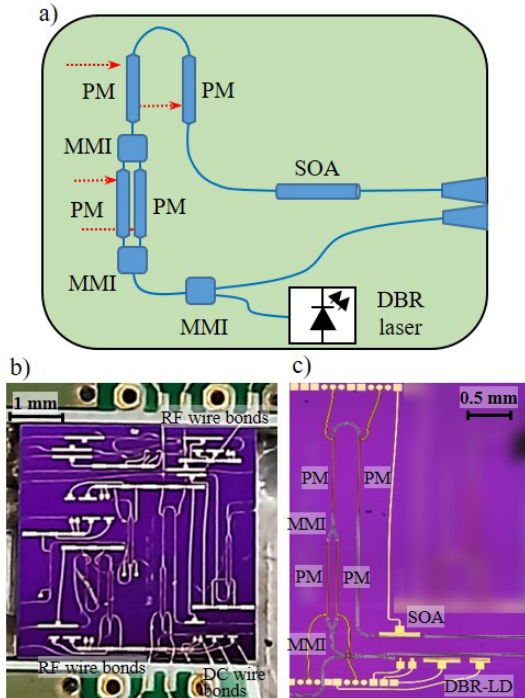


Fig. 1. Photonic integrated circuit. (a) Schematic; (b) and (c) photographs.

In this letter, we experimentally demonstrate a low-phase-noise mm-waves generator based on an integrated optical frequency comb. The OFC-based tenfold-multiplied signal at 26 GHz shows a remarkable low-phase-noise feature, equivalent to the commercially available RF generator used as the comb source, suited for 5G NR wireless transmissions.

II. INTEGRATED OPTICAL FREQUENCY COMB

Fig. 1(a) shows a schematic of the photonic integrated circuit based on cascaded modulators [11], [14] to generate an OFC, which was previously characterized by our research group and reported in [12] and [13]. The device has been realized in an Indium Phosphide multi-project wafer run at Oclaro Technology plc, UK [15] exploiting a generic integration platform. An on-chip distributed Bragg reflector laser diode (DBR-LD) is used as a continuous-wave (CW) light source, however, an external laser source coupled to the PIC input waveguide through a spot-size converter (SSC) can also be employed. The CW signal from either source enters a 2×2 multi-mode interference (MMI) splitter that sends it toward a dual-drive Mach-Zehnder modulator (DD-MZM), inducing an amplitude modulation on the signal. In detail, the MZM is composed of a 1×2 MMI splitter, two 1-mm-long PMs, and a 2×1 MMI coupler. Phase modulators, exploiting the quantum-confined Stark effect, have a 3-dB bandwidth of about 7 GHz and a V_π of about 5 V. The signal then crosses two further 1-mm-long PMs, adding a phase modulation to the signal. Finally, the processed signal is amplified by a 500- μm -long multi-quantum-well SOA and coupled to the output fiber through another SSC. A high-numerical-aperture fiber-array is aligned at the chip edge by means of a micro-positioner.

The realized device has been placed on a metal chuck and connected via wire-bonds to a custom-designed printed circuit board (PCB): four RF ports drive the PMs, while five DC ports

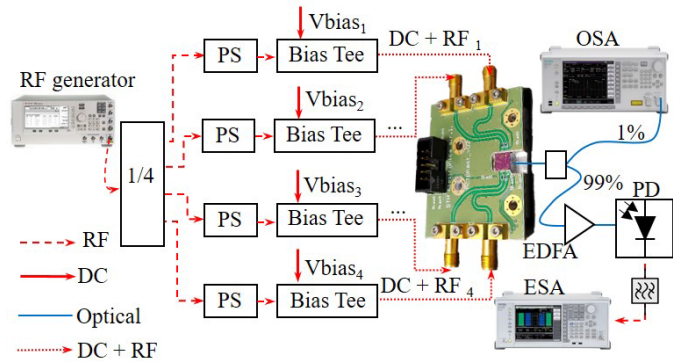


Fig. 2. Experimental setup block diagram for the low-phase-noise tenfold frequency multiplication based on integrated OFC. PS - phase shifter; OSA - optical spectrum analyzer; ESA - electrical spectrum analyzer; PD - photodetector.

feed the DBR sections and the SOA. The chip on the metal chuck surrounded by the PCB is depicted in Figs. 1(b) and (c). The footprint is around $4.5 \times 2.5 \text{ mm}^2$, limited by design constraints concerning the orthogonal placement of PMs and gain sections. The PCB with SMA RF interfaces and GPIO DC interfaces is shown in Fig. 2.

III. EXPERIMENTAL SETUP AND RESULTS

Fig. 2(a) reports the block diagram of our proposed low-phase-noise tenfold frequency multiplication based on an integrated OFC. Our approach focuses on applying the photonic integrated circuit in a centralized radio access network (C-RAN) architecture, aiming to distribute the OFC and to optically generate mm-waves at the remote radio units (RRUs). A 43-GHz RF generator (E8267D PSG from Keysight) provides a 24.7 dBm electrical carrier centered at 2.6 GHz, which is equally divided in four by means of an electrical splitter. The phase of each branch is controlled by a mechanical phase shifter (PS), enabling a proper adjustment on the temporal phase alignment among the PMs, which directly impacts the OFC spectral flatness [14]. Afterward, bias tees have been used for combining the electrical carriers with the required DC bias voltages, feeding the PMs through the SMA connectors. In order to achieve a large number of comb lines and enhanced flatness, the PMs have been driven with V_π multiples, whereas the MZM has been polarized around V_π [16]. The integrated DBR laser and the SOA currents have been set to 70 mA and 55 mA, respectively.

At the PIC output, the power of the optical frequency comb was about -6 dBm . The signal has been then split in two ways: 1% optical power was monitored by an optical spectrum analyzer (OSA), whereas the remaining optical power (99%) reached an Erbium-doped fiber amplifier (EDFA) and then a high-speed photodetector. The EDFA has been used to monitor and control the optical power, ensuring 2 dBm optical power at the photodetector input. Since the OSA even at the narrowest resolution (0.07 nm) cannot resolve the comb spectrum, we have used a heterodyne detection technique to image the OFC, enabling an accurate OFC visualization based on the measured electrical signal, optical spectrum, and photodetector response. Therefore, the 2.6-GHz-spaced optical frequency comb centered at 193.5 THz is presented in Fig. 3. The optical tones extend from 193.4 THz up to 193.6 THz.

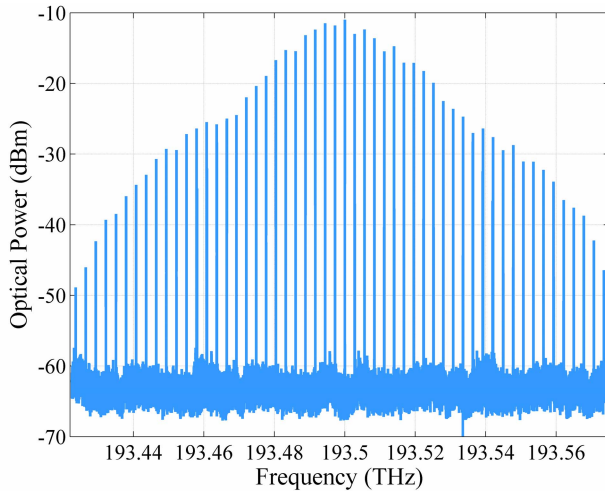


Fig. 3. 2.6 GHz optical frequency comb at the PIC output.

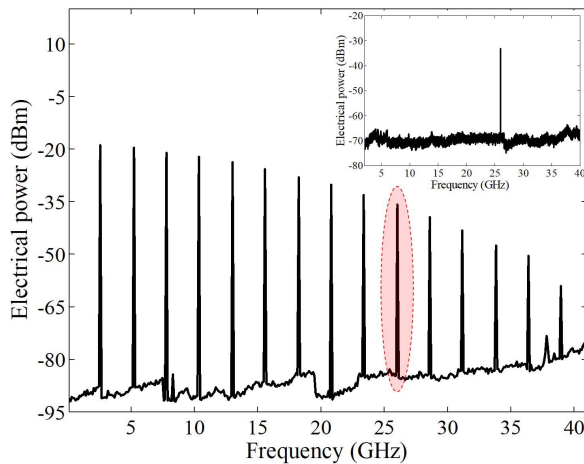


Fig. 4. 2.6-GHz electrical comb at the photodetector output; in the inset the filtered tone at 26 GHz.

One can note 19 tones within a 10 dB intensity range from the maximum optical power, with an optical signal-to-noise ratio (OSNR) higher than 40 dB. Considering the entire comb and the noise floor around -60 dBm, 49 tones provide an OSNR higher than 20 dB, whereas 36 tones present an OSNR higher than 30 dB, which is a typical value from optical transceivers. This achievement demonstrates the applicability of our approach for generating mm-wave signals on a wide spectral range.

The phase-stabilized optical frequency comb lines have been converted into a set of electrical tones by means of a 74-GHz bandwidth photodetector and measured by a 43-GHz electrical spectrum analyzer (ESA), as reported in Fig. 4. A stable electrical comb with a 2.6-GHz repetition rate can be appreciated over the entire frequency range. Furthermore, a high signal-to-noise ratio (SNR) can be observed for all generated harmonics. Therefore, after the photodetection process, the electrical carriers can be properly separated and employed in specific applications, depending on the desired frequency range. Considering a tenfold frequency multiplication, we note a high-spectral-purity mm-wave electrical carrier at 26 GHz.

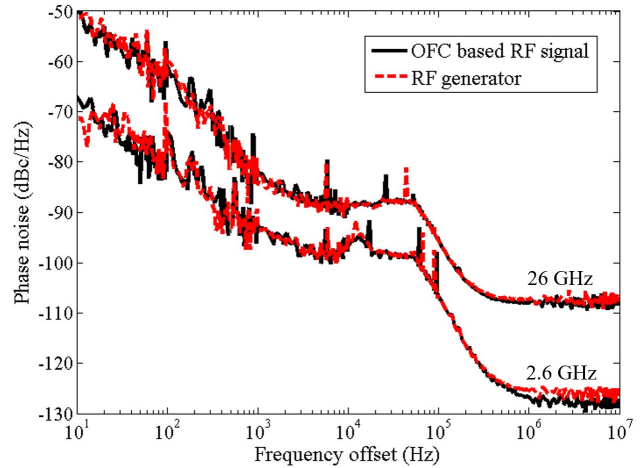


Fig. 5. 2.6 GHz and 26-GHz phase noise comparison between OFC-based signals and the commercial RF generator.

We have used a 1-dB insertion loss band-pass filter (BPF) with 1-GHz bandwidth centered at 26 GHz for isolating the single harmonic as presented in the inset from Fig. 4, since this frequency range has been standardized for 5G mm-wave applications. Indeed, BPFs could improve the system spectral purity, however, they are not mandatory, depending on the application and the required spectral purity, since in a practical scenario the amplifiers, mixers and antennas are developed for a specific frequency range, avoiding undesired frequencies. As expected, the electrical filter selected only the 26 GHz signal, demonstrating a high spectral purity and a significant electrical power of -34 dBm.

In order to validate the low-phase-noise tenfold frequency multiplication based on an integrated OFC, we have measured the OFC-based signal phase noise and have properly compared it with the RF generator used to generate the optical frequency comb. Phase noise measurements are essential in communications systems, enabling to precisely characterize the frequency stability of systems and of oscillators. Fig. 5 presents the phase noise measurements at 2.6 GHz and 26 GHz for both RF generator and our proposed approach. The monolithically integrated OFC source provides phase-stabilized optical lines, as a consequence, frequency multiplication with low phase noise is obtained. Considering the measurements at 26 GHz, we have observed phase noise of around -50 dBc/Hz and -80 dBc/Hz for 10 Hz and 1 kHz offsets, respectively. The OFC-based tenfold multiplication signal (26 GHz) presents a remarkably low phase noise, comparable to that of the commercial RF generator used as its source. The phase noise of the multiplied signal is approximately equal to the RF-driven source phase noise added by $20\log_{10}(m)$, where m is the frequency multiplication factor [9]. Regarding the fundamental frequency (2.6 GHz), we can appreciate a similar phase-noise response, with -70 dBc/Hz and -90 dBc/Hz for 10 Hz and 1 kHz offset, respectively. Therefore, the proposed integrated OFC application enables RF frequency multiplication up to mm-waves, providing a phase noise equivalent to that of the RF source, without adding phase distortions.

The last characterization step consisted in measuring the phase noise for 2-, 4-, 6-, 8-, 10- and 12-times OFC-based frequency multiplication and in comparing with that of the RF generator, demonstrating the system feasibility to generate

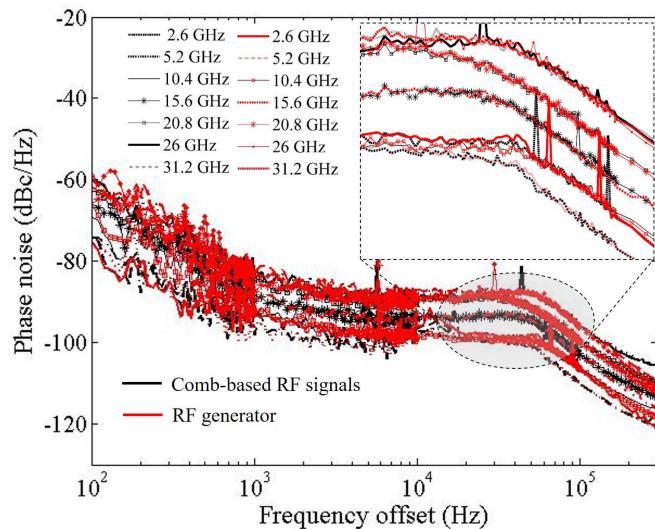


Fig. 6. Phase noise measurements for 2-, 4-, 6-, 8-, 10- and 12-times frequency multiplication compared with the RF generator.

low-phase noise electrical carriers over the entire frequency range. Fig. 6 displays the phase noise measurements at 2.6, 5.2, 10.4, 15.6, 20.8, 26, and 31.2 GHz for both the OFC-based frequency multiplication and the commercial RF generator. Although the phase noise curves present a stochastic response for offsets lower than 1 kHz, no apparent phase distortions occur on the signals obtained by the OFC-based frequency multiplication. Additionally, a zoom-in view for offsets between 10 kHz and 100 kHz allows an accurate comparison. One more time, the OFC-based frequency multiplication provided a suitable phase noise, equivalent to the RF generator measurements at the same RF power. Therefore, the integrated OFC demonstrated frequency multiplication up to 12-times without phase impairments, providing a phase noise equivalent to that of the generator used as the RF source. It is worth mentioning that even higher multiplication factors can be achieved, since we used only 16.5 dBm at each PM modulator input, not requiring electrical amplifiers.

IV. CONCLUSION

We have successfully proposed and experimentally implemented a low-phase-noise tenfold frequency multiplier based on an integrated optical frequency comb generator. The extremely compact integrated OFC generator was fabricated in Indium Phosphide and is flexible in terms of central wavelength and OFC repetition frequency. OFC generation at 2.6 GHz has been reported, in which 36 tones showed an OSNR higher than 30 dB, demonstrating the potential to generate mm-wave signals based on the heterodyne technique. A 74-GHz photodetector enabled a set of 2.6 GHz phase-stabilized electrical tones, reaching up to 39 GHz with a considerable SNR. Phase noise measurements enabled to precisely characterize the OFC-based mm-wave signal frequency stability and compare it with that of the RF generator source. Considering a tenfold frequency multiplication (26 GHz), we have achieved phase noise of -50 dBc/Hz and -80 dBc/Hz for 10 Hz and 1 kHz offsets, respectively. The OFC-based tenfold multiplied signal presented a remarkably low phase noise, equivalent to the commercially available RF generator

used as the source at the same RF power. In addition, the proposed system also demonstrated frequency multiplication up to 12-times without phase impairments and with high spectral purity, validating its use for mm-wave applications over a wide frequency range. Further size, cost and power-consumption reductions are expected by assembling the PIC on a PCB comprising all the needed integrated electronics. Future works regard the PIC use in a real 5G network based C-RAN architecture to distribute and to optically generate mm-waves at the RRU, enabling an OFC-based 5G NR mm-waves access point in accordance to the 3GPP specifications.

ACKNOWLEDGMENT

The authors would like to thank Dr. Marco Chiesa for the support in PIC packaging.

REFERENCES

- [1] P. Popovski, K. F. Trillingsgaard, O. Simeone, and G. Durisi, "5G wireless network slicing for eMBB, URLLC, and mMTC: A communication-theoretic view," *IEEE Access*, vol. 6, pp. 55765–55779, 2018.
- [2] *Base Station (BS) Radio Transmission and Reception*, Standard (TS) 38.104, Version 15.13.0, 3rd Generation Partnership Project (3GPP), Tech. Specification, 3GPP, 2021.
- [3] T. S. Rappaport *et al.*, "Millimeter wave mobile communications for 5G cellular: It will work," *IEEE Access*, vol. 1, pp. 335–349, 2013.
- [4] L. A. M. Pereira *et al.*, "Implementation of a multiband 5G NR fiber-wireless system using analog radio over fiber technology," *Opt. Commun.*, vol. 474, Nov. 2020, Art. no. 126112.
- [5] I. Degli-Eredi *et al.*, "Millimeter-wave generation using hybrid silicon photonics," *J. Opt.*, vol. 23, no. 4, Apr. 2021, Art. no. 043001.
- [6] G. Qi, J. Yao, J. Seregelyi, C. Belisle, and S. Paquet, "Generation and distribution of a wide-band continuously tunable millimeter-wave signal with an optical external modulation technique," *IEEE Trans. Microw. Theory Techn.*, vol. 53, no. 10, pp. 3090–3097, Oct. 2005.
- [7] L. Goldberg, H. F. Taylor, J. F. Weller, and D. M. Bloom, "Microwave signal generation with injection-locked laser diodes," *Electron. Lett.*, vol. 19, no. 13, pp. 491–493, Jun. 1983.
- [8] A. Bordonalli, C. Walton, and A. J. Seeds, "High-performance phase locking of wide linewidth semiconductor lasers by combined use of optical injection locking and optical phase-lock loop," *J. Lightw. Technol.*, vol. 17, no. 2, p. 328, Feb. 1999.
- [9] W. Li and J. Yao, "Investigation of photonic assisted microwave frequency multiplication based on external modulation," *IEEE Trans. Microw. Theory Techn.*, vol. 58, no. 11, pp. 3259–3268, Nov. 2010.
- [10] C. T. Lin, P. T. Shih, J. Chen, W. Q. Xue, P. C. Peng, and S. Chi, "Optical millimeter-wave signal generation using frequency quadrupling technique and no optical filtering," *IEEE Photon. Technol. Lett.*, vol. 20, no. 12, pp. 1027–1029, Jun. 15, 2008.
- [11] M. Imran, P. M. Anandarajah, A. Kaszubowska-Anandarajah, N. Sambo, and L. Poti, "A survey of optical carrier generation techniques for terabit capacity elastic optical networks," *IEEE Commun. Surveys Tuts.*, vol. 20, no. 1, pp. 211–263, 1st Quart., 2018.
- [12] N. Andriolli, T. Cassese, M. Chiesa, C. de Dios, and G. Contestabile, "Photonic integrated fully tunable comb generator cascading optical modulators," *J. Lightw. Technol.*, vol. 36, no. 23, pp. 5685–5689, Dec. 15, 2018.
- [13] F. Bontempi, N. Andriolli, F. Scotti, M. Chiesa, and G. Contestabile, "Comb line multiplication in an InP integrated photonic circuit based on cascaded modulators," *IEEE J. Sel. Topics Quantum Electron.*, vol. 25, no. 6, pp. 1–7, Nov. 2019.
- [14] A. J. Metcalf, V. Torres-Company, D. E. Leaird, and A. M. Weiner, "High-power broadly tunable electrooptic frequency comb generator," *IEEE J. Sel. Topics Quantum Electron.*, vol. 19, no. 6, pp. 231–236, Nov./Dec. 2013.
- [15] M. J. Smit *et al.*, "An introduction to InP-based generic integration technology," *Semicond. Sci. Technol.*, vol. 29, no. 8, Jun. 2014, Art. no. 083001.
- [16] T. Sakamoto, T. Kawanishi, and M. Izutsu, "Asymptotic formalism for ultraflat optical frequency comb generation using a Mach-Zehnder modulator," *Opt. Lett.*, vol. 32, no. 11, pp. 1515–1517, Jun. 2007.